

An Agent-Based Simulation Model to Evaluate Contacts, Layout, and Policies in Entrance, Exit, and Seating in Indoor Activities Under a Pandemic Situation

Md Tariqul Islam, Saurabh Jain, Yijie Chen, Bijoy Dripta Barua Chowdhury^{ID},
and Young-Jun Son^{ID}, *Member, IEEE*

Abstract—The outbreak of the novel coronavirus SARS-CoV2 has dramatically changed the world and has been a severe health threat in 2020 and 2021. In this article, an agent-based simulation model of pedestrian dynamics is proposed for classroom-type indoor spaces (e.g., classroom, auditorium, food court, and meeting room), which will help organizations such as universities to evaluate alternative policies (namely entrance and exit policy, seating policy, and room layout) concerning the contact-caused risk associated with activities in such places during a pandemic situation. In particular, the proposed work focuses on solving the indoor seat allocation and traffic movement problem while practicing appropriate physical distancing measures. The proposed seating policy evaluates the distance of a seat from the doors and pathways facilitating the evaluation of contact-caused risk associated with the pathway and indoor area movement. Various statistics from two perspectives, risk, and logistics, are reported in the simulation results. The risk metrics used in evaluating different policies include average exposure duration and an average number of contacts with others. To develop a highly realistic crowd simulation considering physical distancing and human intervention nature, deadlock detection and resolution mechanisms are incorporated. From this study, it has been observed that the proposed social distancing (SD) seating policy and zonal exit policy can significantly reduce the contact number and exposure duration at a higher occupancy level. The proposed work helps the organizational policymakers to evaluate different policies and ensure the safe operation of the organizations under pandemic situations.

Note to Practitioners—This article was motivated to ensure safer and efficient operations within indoor facilities by evaluating contact-caused risks and entrance/exit policies during a pandemic situation like coronavirus disease (COVID-19). Most of the recent works related to COVID-19 disease propagation focus on the evaluation of disease transmission at an organization level, however, limited studies focus on the operational aspect of indoor

Manuscript received July 29, 2021; revised September 26, 2021; accepted September 30, 2021. Date of publication October 19, 2021; date of current version April 7, 2022. This article was recommended for publication by Associate Editor Y. Li and Editor J. Li upon evaluation of the reviewers' comments. This work was supported by The University of Arizona. (*Corresponding author: Young-Jun Son*)

The authors are with the Department of Systems and Industrial Engineering, The University of Arizona, Tucson, AZ 85721 USA (e-mail: mdislam@email.arizona.edu; saurabhjain@email.arizona.edu; yijiechen@email.arizona.edu; bijoy@email.arizona.edu; son@sie.arizona.edu).

Color versions of one or more figures in this article are available at <https://doi.org/10.1109/TASE.2021.3118008>.

Digital Object Identifier 10.1109/TASE.2021.3118008

facilities within the organization. To bridge this gap, this article utilizes an agent-based modeling approach to model and understand the pedestrian dynamics in the classroom-like facilities considering physical distancing, seat assignment, and entry/exit policies. Comprehensive simulation modeling and analysis allows the amalgamation of real data, including layout, class schedules, seating arrangement, and allowable capacity to perform various what-if analyses under different policies. This article proposes and evaluates seating assignment based on the associated number and duration of contacts during movements in the pathway and entrance/ exit area of a confined space. In addition, this work evaluates different indoor layouts (e.g., classroom, meeting room, and office) and exit policies (e.g., zonal and non-zonal) at different occupancy levels for appropriate decision support. The proposed approach will aid organizations (e.g., educational institutions, corporate offices, and recreational facilities) to evaluate necessary policies (namely entrance and exit policy, seating policy, and room layout) for safe indoor operations with respect to the minimum contact-caused risk associated with the activities. As a future direction, the outputs from the proposed work can be utilized to obtain the realistic input parameters needed for organization-wide disease propagation models, which will provide decision support at an organizational level.

Index Terms—Agent-based simulation, contact-caused risks, coronavirus disease (COVID-19), indoor activities, policy evaluation.

I. INTRODUCTION

AS OF 8th June, 2021, 172.6 million coronavirus disease (COVID-19) cases and 3.7 million deaths have been reported worldwide, of which the United States (U.S.) accounts for 19% of global cases and 16% of deaths [1]. As such, COVID-19 has had a significantly adverse and long-lasting impact on people from all demographics regardless of age, nationality, education level, income, or gender [2]. Although the risk of serious illness caused by COVID-19 increases with age, with the elderly at the highest risk [3], the report of Centers for Disease Control and Prevention (CDC) shows that, during the summer of 2020, in the U.S., people under age 30 accounted for more than 20% of new COVID-19 cases and were observed as more likely to transmit the virus than any other age group [4]. As of mid-April 2020, 94% of the education community worldwide has been affected by the pandemic, representing 1.58 billion children and youth

from pre-school to higher education in 200 countries [5], [6]. Due to the high infectious risk associated with the educational setting and sudden closure of in-person activities, the learning trajectory and knowledge dissemination were disrupted [7]. Following the outbreak of COVID-19, there was a surge in interest in the role and utility of online and hybrid learning. By March 2020, the majority of universities and schools in the United States had transitioned to online courses, and by 2021, they were partially reopening their campuses through in-person or hybrid programs. Obviously, the reopening of universities and schools will bring large benefits to students and the educational sector, however, education stakeholders should weigh the pros and cons of the health risks associated with reopening and make informed decisions [8]. The primary goal of this work is to develop a highly detailed simulation tool to evaluate the contact-caused risk associated with crowd dynamics in different indoor facilities (e.g., classroom, meeting room, cinema, auditorium, and indoor sports facility), which will enable organizational policy evaluations (i.e., entrance and exit policy, seating policy, and seat layout) with respect to associated contact and exposure risks. The article is organized as follows. Section II provides a brief literature review of the previous research methods in COVID-19 disease propagation, pedestrian simulation, and resource allocation during a pandemic situation. Section III elucidates the details pertaining to the simulation model with all necessary features including physical distancing, deadlock detection, and resolution mechanism, and seat selection method introduced in this research. In Section IV, detailed information about the execution of the simulation model is provided, which include the simulation configuration, a description of the statistical information collected from the study, and the numerical results of the simulation. Finally, in Section V, we summarize the findings from the simulation experiments and conclude by describing possible extensions of the proposed work.

II. LITERATURE REVIEW

COVID-19 pandemic has quickly grown to a global phenomenon in 2020. It has surpassed the total number of cases as well as associated fatalities of the virus of similar nature, such as SARS and MERS [9]. Despite the lower mortality rate compared to its closest viral comparators, it has posed a serious threat in terms of community-level transmission. Additionally, with the prevalence of younger people being asymptomatic or having a lower rate of symptoms, the major transmission threat has increased [10], [11]. With the growing number of cases and the increasing volatility of COVID-19 and its declaration as a worldwide pandemic, public health authorities suggest several protective policies to reduce the infectious risk [12]. It is an established fact that the virus that causes COVID-19 is principally spread from human to human by respiratory droplets produced upon coughing, sneezing, or speaking by an infected person [13]. Droplet transmission, responsible for the close contact COVID-19 transmission, is defined as an infection caused by exposure to virus-containing respiratory droplets. To reduce the transmission via. droplets, guidelines to wear masks, practice physical distancing, and periodic sanitization while interacting with others have been issued [14].

The standard physical distance requirements vary between different healthcare organizations and countries. For example, the World Health Organization (WHO) suggests a safe physical distance of at least 3 ft, while indoors requires a greater distance [15], CDC recommends 6 ft [16], and the German government imposes 4.5 ft as the minimum distance [17] to reduce the risk of transmission. Although according to the UK's Scientific Advisory Group for Emergencies (SAGE), current evidence shows that the transmission risk at 1 m of separation could be 2–10 times higher than 2 m of separation [18], the interaction between people is a dynamic process which suggests that crucial factors which such as walking speed and direction and exact behaviors (e.g., seating, talking, and exercising) should be considered for estimating risk.

Another important aspect of virus transmission is the total exposure duration of an individual [19]. Therefore, it is equally important to limit the exposure duration while interacting with others. As the virus transmission risk is highly correlated with the exposure duration as well as physical distance, the time threshold for in-person interaction has been suggested as 5–15 min in most cases, and up to 30 min in limited situations [20]. However, interacting with others maintaining a safe physical distance for a short period of time does not guarantee that one will not get infected. Hence, when public health authorities and the government prepare for different strategies of public facilities reopening, the people-air-surface-space management should be taken into account [21].

Face-to-face operations of the universities posed a serious threat to the community, thus leading the schools and universities to adopt completely virtual or hybrid models of instruction [22]. The need to reduce the concentration of viral particles for a safer indoor environment can be achieved by utilizing several control measures such as improved ventilation, avoiding air recirculation, air cleaning and disinfection, and minimizing the number of people within an indoor environment [23]. However, there are no recommendations pertaining to the specific values that these parameters could possess for the safe operations of an indoor facility [24]. For this article, we did not consider ventilation, air, and surface cleaning factors. In addition to physical distancing, several works have focused on reducing the direct transmission using floor area per person, improvements in the rate of ventilation to control the concentration of viral infection within the indoor spaces [25]. Another aspect for reducing the direct transmission within the classroom setting includes a safer number of students, seating policies that ensure physical distancing, and entry-exit policies for the class to ensure a safe commute. More recently, there are different works on seat allocation problems in combination with the physical distancing measures. Murray [26] devised a social distance seat planning model utilizing spatial optimization. Salari *et al.* [27] proposed a seat selection algorithm that assigns seats to the onboarding passengers based on distance from the door and aisle. Delcea *et al.* [28] used the reverse pyramid boarding method in an agent-based simulation study to minimize health risks during airline boarding. However, the comprehensive policy evaluation (namely entrance and exit policy, and seating policy, seat layout) study for indoor activities analyzing the

pedestrian's crowd behavior while following physical distancing guidelines is much less explored.

In addition to seating policies, many researchers have developed models that simulate the crowd's movement to explore appropriate people density and physical distance. An agent-based pedestrian dynamic model developed by Harweg *et al.* [29] suggests a density of 16 square meters per person to keep the infectious risk under 2%. However, this finding indicates that only around four students are allowed to take a class in a standard classroom, which is not suitable for the real-world scenario. Considering safety, for outdoor areas (e.g., sidewalks and playgrounds), Mohammadi suggests 3.62 square meters per person [30]. In our simulation model, we emphasize the agent movement behavior under certain policies, while allowing minor physical distancing rule violations in the case of any deadlock situation to represent the human intervention nature and realistic crowd flow. There are different deadlock resolution algorithms applied in different research areas depending on system requirements [31], [32]. CDC's guideline suggests one-way circulation in hallways and classrooms to prevent close contacts which can be one potential resolution for a deadlock situation. However, we examine alternative policies in seat selection, entrance, and exit, considering exposure duration, number of contacts, and occurrence of deadlock and resolution concurrently for a classroom operation.

III. SIMULATION MODELING

In this study, the model utilizes the agent-based simulation technique to capture the individual agent interaction and evaluate the exposure risks caused by these interactions. This section provides the purpose (see Section III-A), an overview of the simulation model (see Section III-B), the key characteristics of the agents with parameters, and variables (see Section III-C). Methodologies involving individual agent's mobility, social force model, physical distancing framework, and agent interaction are explained in Sections III-D–III-F, respectively. Finally, Section III-G describes the implementation details of the simulation in terms of seating policy and execution. This section will help ensure the proposed work's scalability to evaluate different policies for different indoor activities. AnyLogic 8.5.1 has been utilized to model and implement individual agent behaviors, and their interactions within the shared environment.

A. Purpose

The purpose of the proposed model is to mimic and evaluate different policies (namely entry and exit policy, seating policy, and seat layout) involving indoor activities, and devise the most appropriate policies, which can minimize the contact-caused risk to the organization in the event of a pandemic. In this work, classrooms have been considered for the case study to ensure the extensibility of the proposed work for other indoor venues (e.g., cinemas, auditoriums, indoor sports fields, seminars, and airlines). Evaluation of policies using the proposed model is primarily based on statistical results of risk and logistics parameters. We utilize total time for all students

TABLE I
AGENTS, PARAMETERS, AND VARIABLES

Agent	Parameters	Variables
Student	Initial seat location, agent diameter, velocity	Agent diameter, deadlock duration, color, start of entrance time, end of entrance time, start of exit time, end of exit time

to leave the classroom (exit time) as the logistical parameter in the model. As the perception of risk varies with the situation, based on the COVID-19 pandemic context, the average amount of time an agent spends within proximity (within 0–3- and 3–6-ft range) of the other agents (i.e., average exposure duration) and the average number of contacts an agent has with other agents is considered for risk evaluation. We also introduced a physical distancing and deadlock resolution framework into the embedded social force model to ensure realistic pedestrian behavior during the simulation. In addition, an automatic social distancing (SD) seat selection algorithm was implemented and tested against the nearest alternate seating (AS) seating algorithm in the simulation model.

B. Process Overview

At the model startup, the initialization parameters (e.g., facility parameters, agent parameters, and agent generation data) are assigned based on modeling requirements from the user. In a pedestrian dynamics' context, the Anylogic pedestrian library [33]–[36], was used to generate student agents that follow the social force algorithm. In the next step, student agents are assigned seats in the classroom based on maximum distance from the doors and pathways. A comparative analysis for the performance of different seat selection methods has been performed to evaluate entrance and exit policies along with their associated contact and exposure duration. During the simulation, physical distancing and deadlock resolution mechanisms have been deployed to ensure a safe and realistic model performance. At the end of the simulation, a dashboard has been designed to provide users with an overview of the output statistics. Finally, the user is given the option to change the input configuration depending on the output statistics to identify the optimal policy and classroom setup.

C. Agents (Parameters and Variables)

The primary focus of the proposed work is to mimic the movement of pedestrians within indoor spaces realistically. Therefore, "student agents" have been used to perform the movements. Table I lists the parameters and variables of the student agent. To define the configuration and setting of the simulation environment, various parameters and variables are considered based on requirements provided by the organization, such as classroom capacity, student agent arrival rate, duration of the class, duration of the break, total entrance time, and total exit time. All the model-relevant information (e.g., class schedule, class time, classroom capacity, classroom dimension, and entrance and exit policy) used in the proposed

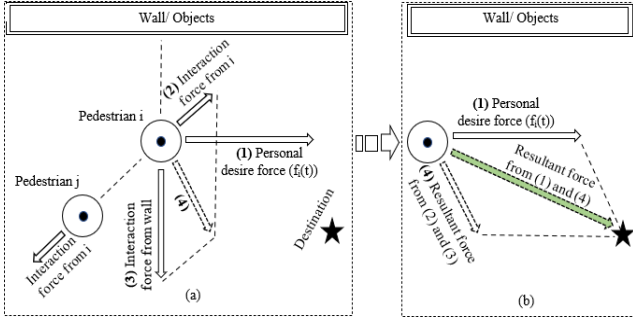


Fig. 1. Different force components: (a) interaction and personal desire force and (b) resultant force of social force model.

work was provided by concerned university authorities to represent the classroom environment.

D. Social Force Model and Pedestrian Library

Student agent behavior was modified within the Anylogic pedestrian library by modeling physical distancing and deadlock detection and resolution mechanisms, and was used to assess capacity and throughput, identify bottlenecks caused by pedestrians, and execute planning within a public area. The movement of the pedestrians within the environment is governed according to the social force model [37]. Each agent within the simulation utilizes the shortest path to perform the movement and avoid collisions with other objects (e.g., walls, desks, and other pedestrians). The pedestrian behavior is defined using a block diagram, which specifies the movement patterns and destinations across space. The physical environment is comprised of the space markup elements such as walls, service points, and attractors.

To prevent the uncoordinated movement of pedestrians, a realistic social force model including individual physical and psychological characteristics and the collective herd instinct is employed in this study. The main components of the social force are: 1) pedestrian's self-consciousness; 2) force from other pedestrians; and 3) force from the environment (walls, doors, and objects) (see Fig. 1).

The governing equation for the social force model implemented in the pedestrian library is as follows [23]:

$$m_i \left(\frac{dv_i}{dt} \right) = m_i \left(\frac{v_i^0(t)e_i^0(t) - v_i(t)}{\tau_i} \right) + \sum_{j \neq i} f_{ij} + \sum_W f_{iw}. \quad (1)$$

Pedestrian's behavior is depicted by desired speed ($v_i^0(t)$), desired direction ($e_i^0(t)$), actual speed ($v_i(t)$), and interactions with other pedestrians (f_{ij}), walls and objects (f_{iw}). To better understand the forces acting on the pedestrian *j*, we developed two diagrams that illustrate the forces and their resulting vectors. The first term on the right side of (1) represents the pedestrian's self-consciousness [force component (1) in Fig. 1(a)], while the other two terms represent the interaction force from other pedestrians [force component (2) in Fig. 1(a)], walls, desks, and objects [force component (3) in Fig. 1(a)]. Force component (4) in Fig. 1(a) is the resulting force of (1) and (2). The green dotted arrow in Fig. 1(b) represents the resultant force (1) and (4), which guides the agent to its destination.

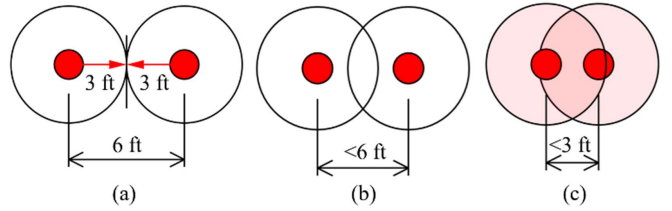


Fig. 2. Physical distancing at (a) 6 ft (b) less than 6 ft but greater than 3 ft, and (c) less than 3 ft (violation of distancing rule) distance range.

E. Physical Distancing

Physical distancing, also called "SD," means keeping a safe space between two individuals belonging to a different cohort. It has been one of the essential factors and practiced policies during the COVID-19 outbreak due to its effectiveness in reducing disease transmission among humans [38]. In a regular setting, efficient conduct of daily activities often requires in-person interaction among individuals of different ages, races, and genders. This is why it is essential to maintain physical distancing with other daily preventive measures in all environments and activities involving people.

The concept of physical distancing has been a focus area in recent works due to the high volatility, high contact-based spreading, and mortality rate of the COVID-19 virus. Correspondingly, in simulation modeling, physical distance is a new field and can provide a significant contribution to the original Social Force Model.

In this work, we introduced a new physical distancing framework to ensure a safe boundary between student agents. While most public health officials recommend a 6-ft distance between people, a review of 172 studies from 16 countries concluded that a 3-ft distance is effective with proper face masks and other safety measures [39]. Another study on 251 school districts of Massachusetts public school districts, encompassing 540 000 students and 100 000 K-12 staff, who attended a 16-week in-person learning program did not show a significant difference in the number of Covid-19 cases under 3 ft of SD, as opposed to 6-ft measures [40]. In light of these studies, the nation's top infectious disease experts are planning to validate three feet of SD as the safety measure for reopening schools in the coming days [41]. So, in this study, we considered 3-ft mandatory physical distancing policy considering proper face masks and a sanitized classroom environment.

In this work, the physical distance has been implemented by dynamic changes in the agent's diameter during interaction with other agents illustrated in Fig. 2. Each student agent ensures a 3-ft physical distance from others in the class environment [Fig. 2(a) and (b)]. Whenever someone comes within 0–3 ft of a student agent, that student's distance measure is violated, and the physical distancing circle turns red [see Fig. 2(c)]. As the modeled environment represents a classroom where the majority of the students are in the mid-20s, a 0.65-ft radius cylinder (i.e., 1.3-ft diameter) has been considered for each student agent to represent the average human shoulder width [42]. In addition, for the visual representation of an agent, a dummy cylinder of the size of the student agent was considered.

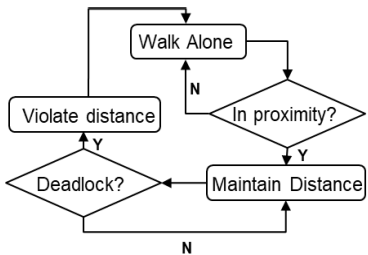


Fig. 3. Physical distancing and deadlock resolution (human intervention) flowchart.

When moving in a virtual environment, the student agent constantly searches its surroundings [see Fig. 3] to detect any other student agents within a radius of 3 ft (6 ft in diameter), thus violating the physical distancing constraint. As a result, the diameters of the agents increase to 3 feet from 1.3 feet whenever another student is inside that 3-ft radius (6-ft diameter) zone. However, visualizing a change in the size of a human body due to interaction is implausible. To avoid this, we used the constant dummy cylindrical circle as a visual representation while changing the actual agent diameter and hiding it from the simulation screen. Due to the default social force, this diameter change in agent size results in a body compression and sliding friction force by impeding the tangential motion of the agents. As a result of this force, both agents move away from each other and maintain a 3-ft physical distance in the simulation. Eventually, by changing the agent's actual diameter in the simulation, we use the inherent social force to exert a repulsive force that pushes the agents apart but keeps the visual representation (dummy diameter) of the agent the same as before.

The problem occurs in a classroom-like environment, where many obstacles, such as walls, desks, and chairs are present. Analogous to the interaction force between pedestrians, physical objects also trigger interaction forces on student agents when the agent body is close to the obstacles. This leads to sudden changes in agent diameter due to physical distance violation, thus causing instability in the agents' movement due to dynamically changing distance from other agents and objects. For example, with a repulsive force applied to push the student agent backward, the student agent may also get a forward push if there are other obstacles near the backward direction. This eventually leads to repeated push and vibrations. Suppose the student agent moves in a congested environment surrounded by walls and objects. In that case, this instability will be exacerbated by repeated changes in diameter, which is common in classroom-like environments.

Since the pedestrian library of AnyLogic 8.5.1 was not developed for physical distancing modeling, because of the sensitivity of the social force algorithm used in the library, the model does not perform well when the agent diameter increases and changes to 3 ft (which is unreasonable for a human diameter). To overcome these challenges, we incorporated the following approaches:

1) Different Scaling: In AnyLogic, the scaling ratio is set as the ratio of the animated pixels to the physical unit of length. In the simulation, we specify the unit of length to pixel correspondence to represent the object of the real world.

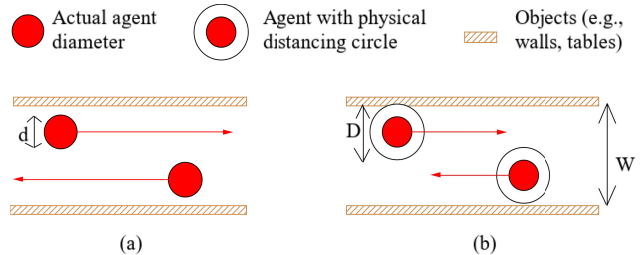


Fig. 4. (a) No deadlock. (b) Deadlock without violation of physical distancing.

Usually, the scale is set to a fixed unit at both the animation level and agent level. To overcome the unrealistic crowd behavior caused by the diameter change, we used different scales in the main simulation interface (animation scale) and the student agent (actual pedestrian scale) in our model. However, we increased the student agents' diameter by the factor of scale ratio to maintain consistency in both simulation main and student agent. By implementing this scaled-down method in the student agent, we generated realistic crowd movement behavior throughout the simulation.

2) Time Step: By setting the time step parameter to lower values, simulation can track student agents' movement more precisely. We used a time step of 0.05 s in the simulation, which enabled a smooth student agent movement but made the model computationally expensive.

F. Deadlock

It is imperative to represent a realistic movement of students within the classroom setting. The dynamic changes in the diameter of the pedestrian cylinder in a social force model often led to blocking or deadlocking the pedestrian movements in narrow pathways if a resolution mechanism is not provided explicitly. Hence, in order to represent realistic human intervention nature, it is important to devise a resolution technique to handle deadlock situations. Deadlock is one of the commonly used situations in distributed simulation, automated manufacturing systems, and communication networks. A deadlock occurs when a group of processes intends to acquire the same resource, but the resource requests cannot be satisfied due to the limited resource. In our work, initially, we have observed some deadlock situations within the narrow pathways of the classroom. So, we devised a deadlock detection and resolution methodology to represent more realistic student movements (e.g., human interventions).

A deadlock could occur in our simulation model due to a scarcity of the resource pathway space. Due to the abundance of desks and chairs, and physical spacing requirements in the classroom, the classroom space is packed, and students' movements are more restricted than the non-pandemic situation. When student agents moving in opposite directions intend to pass each other on a narrow path while adhering to the physical distancing requirement, a deadlock situation may arise. Suppose the pathway width (W) is less than the sum of both agents' physical distancing circle diameters (D). In that case, the student agents will not pass each other due to physical distancing restrictions, resulting in a deadlock [see Fig. 4(b)]. However, if there were no physical distancing restriction in the

model, students' agents would be able to move freely without experiencing any deadlock since the pathway width (W) is more than the total of actual agent diameter (d) [see Fig. 4(a)]. As such, deadlock situations would rarely occur for non-pandemic scenarios, without requiring physical distancing. For pandemic scenarios, the deadlock may occur, and our detection and resolution algorithm is applied to represent the real human intervention behavior.

In some situations, a wide pathway can also create a deadlock situation due to multiple student agents' presence at the same time. Therefore, it is important to understand and devise a deadlock resolution technique to model realistic pedestrian behavior. In the simulation model, most of the space is occupied by the physical distancing circle of each agent. One feasible solution to avoid a deadlock situation is by disabling the physical distancing algorithm for a particular instance to allow both student agents to share the available pathway space. The first step of this deadlock resolution is to identify a deadlock situation. A deadlock situation cannot be declared when an agent is not moving for a certain duration. Hence, simply labeling zero velocity as a deadlock situation will misclassify a student seating in the chair as deadlock. In this model, deadlock logic was formulated by considering several information during the simulation runtime including the time of the incident (namely class time or break time), the number of student agents involved in the situation, the width of the pathway, and the number of time agents spent in the stagnant situation. The combination of all the information provided insights to accurately classify the deadlock instance and facilitate the participating agents to turn off the physical distancing mechanism for that specific moment (i.e., human intervention nature in a real-world setting).

G. Evaluation of Seat Choice Algorithms

Another important aspect investigated in this research is to find an optimal seating policy by minimizing the possible number of contacts and exposure in a classroom environment. Thus, we have tested two different seating methods in our simulation under different policies and classroom setting to find the best seating arrangement. The performance of seating policies was evaluated based on three types of simulation output: exit time, average exposure duration, and the average number of contacts.

Different room configurations have been considered for testing seat selection policies. In order to represent the general functional room of educational institutions, GITT129B from the Ina A. Gittings Building at the University of Arizona is used as a case study in this section. We considered this regular classroom and tested different layouts (e.g., collaborative and traditional) and exit policies (zonal exit and non-zonal exit) for different occupancy levels.

The data pertaining to the dimensions of the classroom, desks, chairs, width of the pathways, the distance between seats, location, and the number of entrances and exits, teacher's corner, and available technologies were considered to design the classroom within the simulation. Once the appropriate layout and design have been implemented, the seats for seat selection evaluation must be labeled prior to testing

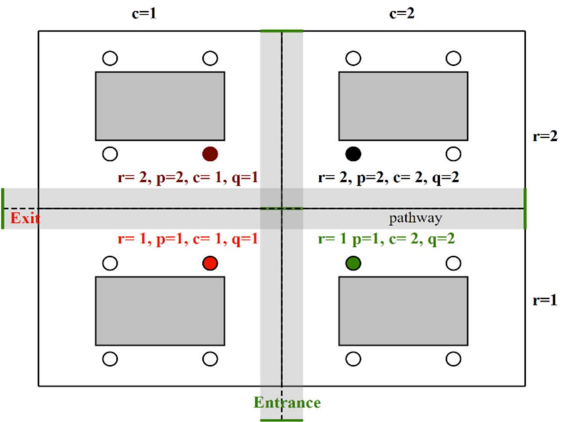


Fig. 5. Seat labeling.

different policies. Hence, the appropriate notations have been formulated to devise a unique label for each seat within the classroom.

The notations for seat labeling are shown as follows.

r, r' = row number of the seat, $\forall r, r' \in R$.

p, p' = upper or the lower sections of the corresponding row.

$p, p' = 1$ represents upper section and, $p, p' = 2$ represents the lower section.

c, c' = column number of the seat, $\forall c, c' \in C$.

q, q' = right or left side of the corresponding column
 $q, q' = 1$ represents right side and $q, q' = 2$ represents the left side.

R = Set of rows, $\{1, 2, 3, \dots\}$, based on classroom layout.

C = Set of columns, $\{1, 2, 3, \dots\}$, based on classroom layout.

Fig. 5 shows the seat labeling procedure through visual illustration. Spatially, the black-colored seat has the row value ($r = 2$) and column value ($c = 2$), alternatively black colored seat is located at the intersection of the 2nd row and the 2nd column. The next step is to locate the seat (e.g., right, or left side of the column and upper or lower section of the corresponding row) based on positional value from the corresponding column and row. For example, the black seat is on the lower section of the row ($p = 2$) and the left side of the column ($q = 2$). So, that black seat can be labeled as ($r = 2, p = 2, c = 2, q = 2$). Similarly, the green seat can be labeled as ($r = 1, p = 1, c = 2, q = 2$).

The distance values have been derived by using the Euclidean distance formula between two seats by using the following equation:

Euclidean distance,

$$D = \sqrt{(X_{r,p,c,q} - X'_{r',p',c',q'})^2 + (Y_{r,p,c,q} - Y'_{r',p',c',q'})^2}. \quad (2)$$

Based on the unique labels generated for each seat within the classroom, two-seat selection policies have been tested in this study: 1) proposed SD seating and 2) AS seating.

1) *Seat Selection Method 1: SD Seating*: This article proposes a seating policy to make appropriate seat assignments

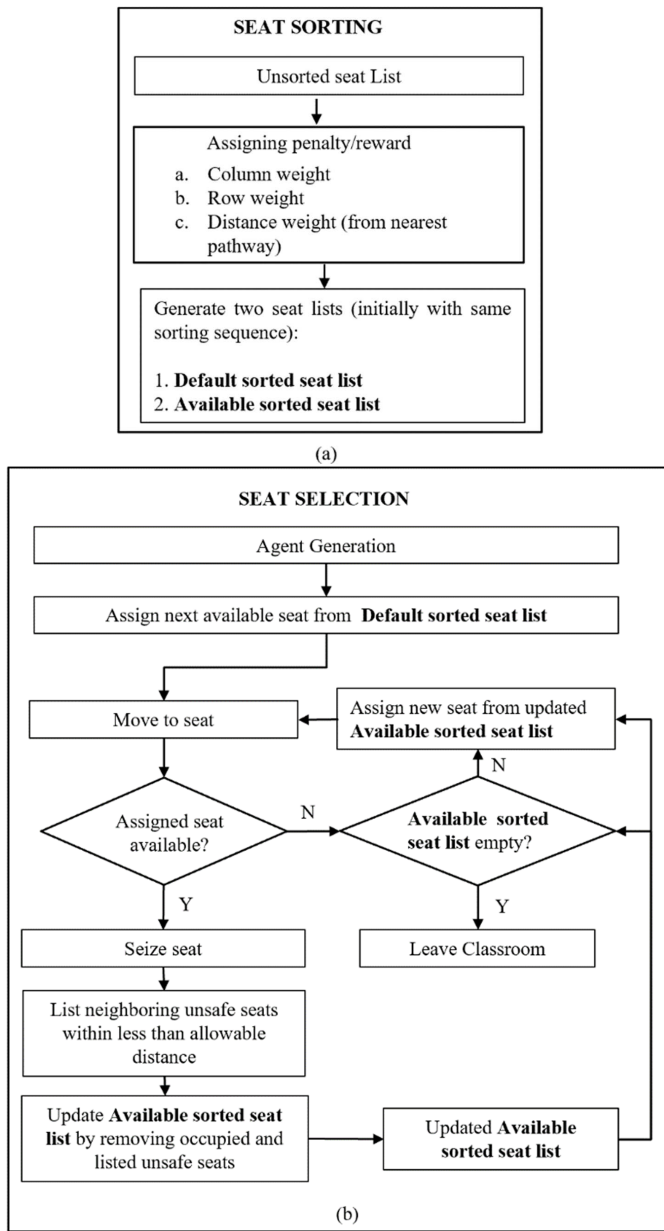


Fig. 6. (a) Seat sorting, (b) SD seat selection algorithm.

to students to ensure the appropriate SD while attending the class. The policy works by associating penalty value to each seat based on the distance from entrance and exit doors and distance from the nearest pathway.

Seats located near the doors are subject to higher penalties because these seats are close to the entrance or exit door and have a higher potential for contact and exposure. Conversely, seats from the farthest corner of the classroom are least penalized due to the lower contact and exposure risk because of their location.

The proposed SD seating policy consists of two segments: seat sorting and seat selection. As shown in Fig. 6(a), all seats are sorted based on the column, row, and distance weights on model startup. Initially, the same sorted seat list was used to create two identical seat lists (default sorted seat list, available sorted seat list). Sorting is based on a seat's desirability: the

seat with the lowest penalty is at the top and the seat with the highest penalty at the bottom). Seats were assigned to the students from the default sorted seat list upon creation based on the first come first serve basis.

As the student agent's seat is assigned, the student goes to the designated seat by following a 3-ft physical distancing guideline. On arrival to the seat location, each agent confirms whether the assigned seat from the “default sorted seat list” is also available in “available sorted seat list” Fig. 6(b). If the seat is available in both lists, the student agent occupies the allocated seat and the ‘available sorted seat list’ is updated by removing the occupied seat. Furthermore, upon arrival at the assigned seat, the algorithm immediately searches for the other available seats in the area that violates the 3-ft distancing rule. Once those distance violating seats are listed, all of them are subsequently removed from the “available sorted seat list.” Eventually, all the seats will be either assigned or removed by the algorithm due to the physical distancing measures and once the “available sorted seat list” is empty, the new students will be advised not to enter the classroom due to the unavailability of safe seats.

2) Seat Penalization: The rows or columns with a smaller Euclidean distance from the doors possess a higher penalty for potentially high exposure risk and physical distancing violation as those seats to have high pedestrian contact potential. To address this effect, we introduce β_r , γ_c , $\delta_{(r,c)}$ as weights to address the importance of minimizing the number of students on seats closer to the door area.

Here, β_r is the penalty imposed on a desk in row r due to the presence of an entrance or exit door in parallel to that row. γ_c is the penalty imposed on a desk in column c due to the presence of an entrance or exit door in parallel to that column. $\delta_{(r,c)}$ is the average penalty imposed on a desk due to the presence of an entrance or exit door in parallel to that row and/or column.

Consider a classroom with a single door that serves as both an entrance and an exit for all the students. The door is located near and in parallel to the first row ($r = 1$). So, the distance between the door and the rows increases with the increase of row numbers (e.g., $r = 2, 3, 4, 5$). Intuitively, students seated on the first row ($r = 1$) will have a higher probability of getting in contact with entering students than the students seated in the rows of higher value (e.g., $r = 2, 3, 4, 5$). So, β_r should be inversely proportional to the row number or $\beta_r \propto (1/r)$. Similarly, considering an entrance/exit door near and in parallel to the first column ($c = 1$), γ_c should be inversely proportional to the column number or $\gamma_c \propto (1/c)$. Now, if there are two doors in a classroom, one near and parallel to the first row ($r = 1$) and the other close and parallel to the first column ($c = 1$), the overall penalty of a desk position should be proportionate to the average of the associated row and column penalties

$$\delta_{(r,c)} \propto \frac{\beta_r + \gamma_c}{2}. \quad (3)$$

Scenario 1: Some doors are utilized more frequently than others in certain scenarios, prompting the application of a higher penalty weight to some doors. If we consider a door

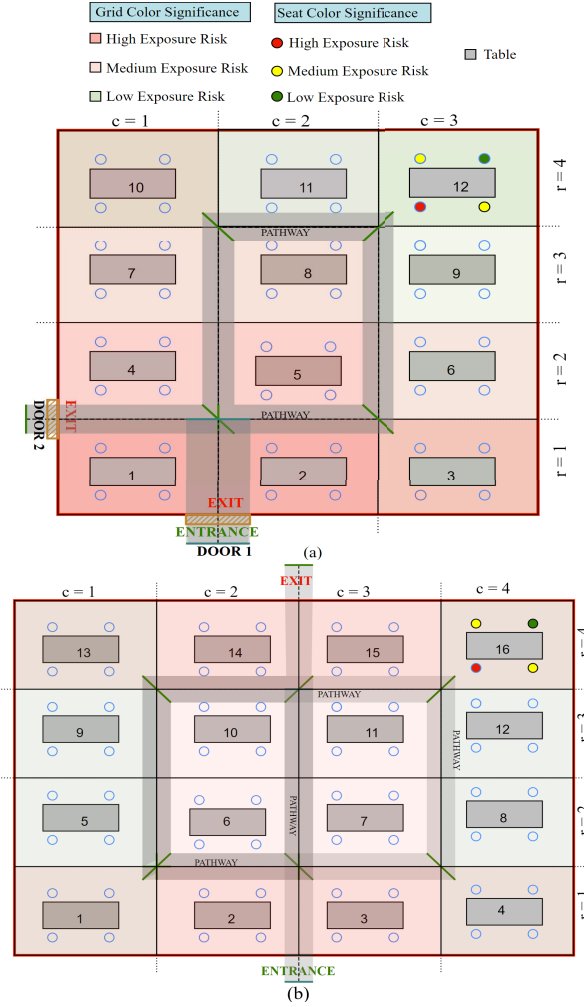


Fig. 7. SD seat penalization and seat selection for different door settings. (a) Layout 1. (b) Layout 2.

[see Fig. 7(a)] near and parallel to the first row (door 1), which is more frequently used for entrance and exit operations than the door in parallel to the first column (door 2), which is only used for exit operations, intuitively we should assign a higher penalty to the seats located near door 1 than door 2. To address this issue, we took the following approach:

$$\beta_r = \left(\frac{1}{r} \right)^{\frac{1}{\theta_1}}, \forall r \in R, \theta_1 \in Z^+ \quad (4)$$

$$\gamma_c = \left(\frac{1}{c} \right)^{\frac{1}{\theta_2}}, \forall c \in C, \theta_2 \in Z^+. \quad (5)$$

We can use this method to assign different penalty weight factors based on a desk's row and column positions. For instance, in this case [see Fig. 7(a)], the location of desks 2 and 4 can be considered. At first look, it may appear that both desks should have the same penalty factor because they are adjacent to the door. Desk 2 should, however, have a greater penalty and so be less desirable than desk 4 because door 1 is utilized more frequently than door 2. This requirement can be easily addressed by considering different values for θ_1 and θ_2 . The direction toward which the room has higher traffic flow should have a higher θ value compared to the direction toward which the room has lower traffic flow.

TABLE II
SEAT PENALIZATION SCORE (β_r, γ_c)

Row (r)/ Column Number (c)	$\theta = 5$	$\theta = 10$
1	1	1
2	0.870550563	0.933032992
3	0.802741562	0.89595846
4	0.757858283	0.870550563

Since door 1 has higher traffic flow in columnwise direction (between columns 1 and 2), we consider $\theta_2 = 10$ to calculate columnwise penalty γ_c and consider $\theta_1 = 5$ to calculate rowwise penalty factor β_r .

For desk 2, $r = 1, c = 2$, so we get: $\beta_1 = ((1/1))^{(1/5)} = 1, \gamma_2 = ((1/2))^{(1/10)} = 0.933$. So, from (3), $\delta_{1,2} = (1 + 0.933/2) = 0.966$.

For desk 4, $r = 2, c = 1$, so we get: $\beta_2 = ((1/2))^{(1/5)} = 0.871, \gamma_1 = ((1/1))^{(1/10)} = 1$. So, from (3), $\delta_{2,1} = (0.871 + 1/2) = 0.935$.

So, for desk 2 we are getting penalty factor 0.966 whereas for desk 4 penalty factor is 0.935. So, desk 2 is more penalized and thus less desirable than desk 4. Similarly, we can get the penalty factors for other desks from Table II as above. From Table II, we get an order of desk's desirability shown as D (desk number): PF (penalty factors from low to high): D(12): PF(0.826), D(11): PF(0.845), D(9): PF(0.849), D(8) PF(0.868), D(10): PF(0.879), D(6): PF(0.883), D(7): PF(0.901), D(5): PF(0.902), D(3): PF(0.948), D(4): PF(0.936), D(2): PF(0.966), D(1): PF(1).

Scenario 2: Consider another scenario [see Fig. 7(b)], in which a room has two doors, one of which is near and parallel to the first row ($r = 1$) and the other of which is near and parallel to the last row ($r = 4$). In this case, the rowwise penalty for rows 1 and 2 should be the same as row 4 and row 3, respectively. The penalty equation for each desk's row position will thus be

$$\beta_r = \left(\frac{1}{r} \right)^{\frac{1}{\theta_1}}, \quad \forall r \in R \setminus \{r \geq r'/2\}, \theta_1 \in Z^+ \quad (6)$$

$$\beta_r = \left(\frac{1}{(r' + 1) - r} \right)^{\frac{1}{\theta_2}}, \quad \forall r \in R \setminus \{r \leq r'/2\}, \theta_2 \in Z^+. \quad (7)$$

Here, $r' =$ maximum row value (for this example, $r' = 4$).

Similarly, if the doors were parallel to the first and last columns, we may write a similar equation for columnwise penalty γ_c and determine the weighted penalty $\delta_{(r,c)}$ from (3)

$$\gamma_c = \left(\frac{1}{c} \right)^{\frac{1}{\theta_3}}, \quad \forall c \in C \setminus \{c \geq c'/2\}, \theta_3 \in Z^+ \quad (8)$$

$$\gamma_c = \left(\frac{1}{(c' + 1) - c} \right)^{\frac{1}{\theta_4}}, \quad \forall c \in C \setminus \{c \leq c'/2\}, \theta_4 \in Z^+. \quad (9)$$

Here, $c' =$ maximum column value (for this example, $c' = 4$).

In the demo classroom settings, a graphical representation of seat preference with the help of color grading has been shown in Fig. 7(a) and (b). In the room [see Fig. 7(a)],

we have an entrance on the lower-left corner and an exit on the left. The aisle (pathway) surrounds the classroom. The seats nearest to the door area are more prone to exposure due to the frequent movement of the student agent in that area. Hence, the model divides the room into blocks based on rows and columns. As shown in Fig. 7(a), the door-side blocks are more reddish, and when we move from the lower-left corner to the right or up, its color will gradually disappear. It can be easily understood that the lower-left corner block is at a higher exposure risk, while the upper right corner block is at a relatively lower risk.

The penalty for a specific row and column intersecting desk is described in the seat penalty section above. Now, considering a particular desk (e.g., upper right corner), there are multiple seats, and the model ranks them according to the distance from the closest path. Understandably, the seat closest to the aisle (red) should have the most exposure and thus rank lowest, while the seat with the greatest distance should have the least exposure (green) and thus rank highest. So, the proposed model iterates through all desks, ranks them based on row and column penalty factors, and then ranks individual seats within a desk-based on pathway distance. Then, when a student agent enters the classroom, the student will be allocated a seat from the ranked seat's list in order of highest to lowest based on availability.

3) Seat Selection Method 2: As Seating: The AS seating policy was tested in the simulation model to compare the risk associated with this policy against our proposed SD seating. In this policy, every alternate seat is assigned to the incoming student based on the shortest distance from the entrance door. The classroom simulation in this study has two entrance doors on the front side of the room and a teacher's desk in the front half of the room. A study shows that [43], the student learns better when they seat in proximity to the teacher compared to the distant seat position. So, it is imperative to analyze the nearest seat policy in this study. It ensures proximity to the teacher facilitating a good learning environment and represents a real-world classroom situation. To minimize contact among students, we removed every alternate seat in this seating policy. In the AS policy, the simulation uses Anylogic's default Dijkstra's algorithm to find the shortest path from the entrance to a seat [44], [45]. The shortest route between two nodes is calculated using Dijkstra's algorithm. The first node represents the student's entrance door, while the second node denotes the student's seat location. When a new student agent arrives at the entrance door, this algorithm sorts all the available seats based on the shortest distance from that specific door and assigns the nearest seat to the student. Once the student sits on that designated seat, the AS algorithm removes the next seat to ensure a safe classroom environment. Eventually, this algorithm finds the nearest seat from the available seat list and assigns it to the new student when the next student arrives.

IV. SIMULATION CONFIGURATIONS, RESULTS, AND VALIDATION

A. Simulation Configuration

Different simulation configurations facilitate the verification and validation of a simulation model. Hence, in the proposed

TABLE III
SIMULATION CONFIGURATIONS

Properties	Configurations
Layout	a. Traditional (Fig. 8 (a)) b. Collaborative (Fig. 8 (b))
Facility type	a. Regular classroom (Fig. 8 (a), (b)) b. Meeting room (Fig. 8 (f)) c. Auditorium (Fig. 8(e)) d. Athletics (dance class, Fig. 8 (d))
Exit rule	a. Zonal (Fig. 8 (b)) b. Non-zonal (Fig. 8 (c))
Maximum allowable capacity	a. 50% (132 students) b. 19 % (50 students)
Seat choice policy	a. SD policy b. AS policy

work, the most important aspect of the validation process for different indoor settings is to test the model under different simulation configurations. The tested simulation configurations are shown in Fig. 8 and described in Table III.

Different types of coursework require different nature of classroom parameters such as classroom type and maximum allowable occupancy of the class. For instance, in a collaborative classroom, students can sit around the workstation, facilitate group discussions, collaboration, and actively participate in the learning process. Conversely, traditional classrooms allow the student to have a good view of the front of the room and enable the instructor to control the students. Correspondingly, depending on the need, a room can be used as a classroom, meeting room, office room, auditorium, or athletic program (e.g., dance class). All these rooms have different use cases, different numbers of entrances and exits, and different numbers of seats depending on the room's functionality. Hence, our model was tested on all these various configurations of facilities to ensure validity, robustness, and assistance to the university policymakers.

During the exiting movement of the crowd, close contact or interaction between student agents will increase the risk of viral infection. Globally, there is increased awareness of imposing different door entry and exit rules to reduce the cross-contact among people. Across the country, many large supermarkets, restaurants, and office buildings have adopted this rule by restricting entry and exit policies. Correspondingly, for the flow of large crowds in and out of theaters, classrooms, meeting rooms, prayer rooms, and auditorium-type places, it can be a good strategy to divide the entire space into different zones and utilize zonal policies for entering and exiting into the indoor spaces. Individuals from a zone will move toward the next zone or exit only if the next zone is empty. By doing this, we can avoid congestion near exit areas and reduce contact among people.

In the context of the pandemic, there are increasing concerns about the maximum allowable occupancy level of a given facility. In some states within the U.S., up to 50 people were allowed to participate in a program with proper physical distancing measures [46]. For educational institutions, flexibility to allow 50% of the total capacity by following mandatory physical distancing and face mask measures has



Fig. 8. Tested simulation configurations as described in Table III.

been considered in some states [47]. Therefore, in our study, we considered two different occupancy levels (maximum 50 attendance, maximum 50% capacity) for different simulation configurations. The proposed SD seating also provides an additional feature of evaluating the maximum allowable occupancy by following mandatory physical distance and masking measures. The maximum allowable occupancy may vary for the same facility due to seating arrangements, the number of entrances and exits, and door locations.

We put our models through rigorous testing using various simulation configurations. It is important to test different seating policies against different simulation configurations in order to obtain relevant statistics associated with the corresponding seating policy. In this article, we investigated SD policy in both traditional and collaborative settings and AS policy in collaborative settings. The initial configuration of the simulation model is shown as follows.

- 1) Fixed Configurations:
 - a) Facility type: Regular classroom.
 - b) Class occupancy: 264, Class duration: 50 min, Class time: 8.00 am.
- 2) Experimented Configurations:
 - a) Layout: a) Collaborative and b) traditional.
 - b) Exit rule: a) Zonal and b) non-zonal.
 - c) Maximum allowable attendance: a) 50% (132 students) and b) 19% (50 students).
 - d) Seat choice: a) SD policy (collaborative and traditional) and b) AS policy (collaborative).

B. Simulation Results

The proposed simulation model was set up and data was analyzed for different configurations of classroom type, allowable occupancy, exit policy, and seating policies. In addition to the various exit and seat selection configurations, we have considered some fixed configurations for testing the policies and analyzing their impacts. Fixed configurations of the classroom include layout factors that could be used to decide the

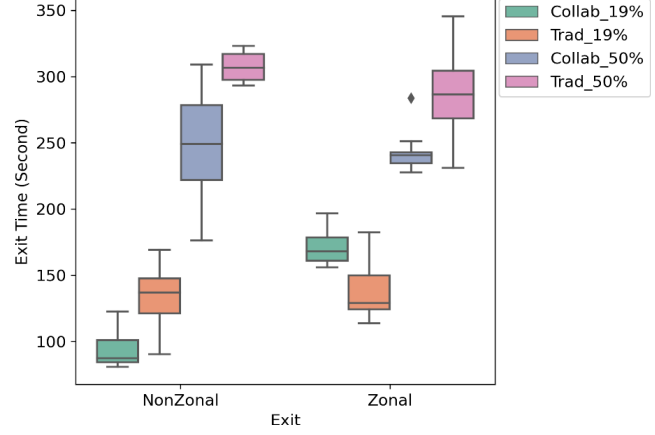


Fig. 9. Average exit time boxplot for different simulation configurations.

appropriate placement of desks. The model layout presented in this study includes collaborative, and traditional seating arrangement. Statistics discussed and analyzed in this section for collaborative and traditional classroom settings are specific for the layout used in the simulation. However, the model framework presented in this study can be easily modified for different layouts and thus can be utilized to study different indoor configurations.

1) *Exit Time*: Exit time is one of the most important factors in order to decide the appropriate break time to allow students of the previous class to safely exit and students of the next class to enter the classroom. Hence, the analysis of exit time for a different type of simulation configuration plays a vital role in the identification of the best policies. The boxplot in Fig. 9 conforms to our intuition of a lower exit time for 19% occupancy compared to the case of 50%. Collaborative classrooms work uniformly better than traditional settings except for the zonal exit with 19% occupancy. Interestingly, the exit time with traditional settings and 19% occupancy is not affected much by the exit policy compared to collaborative

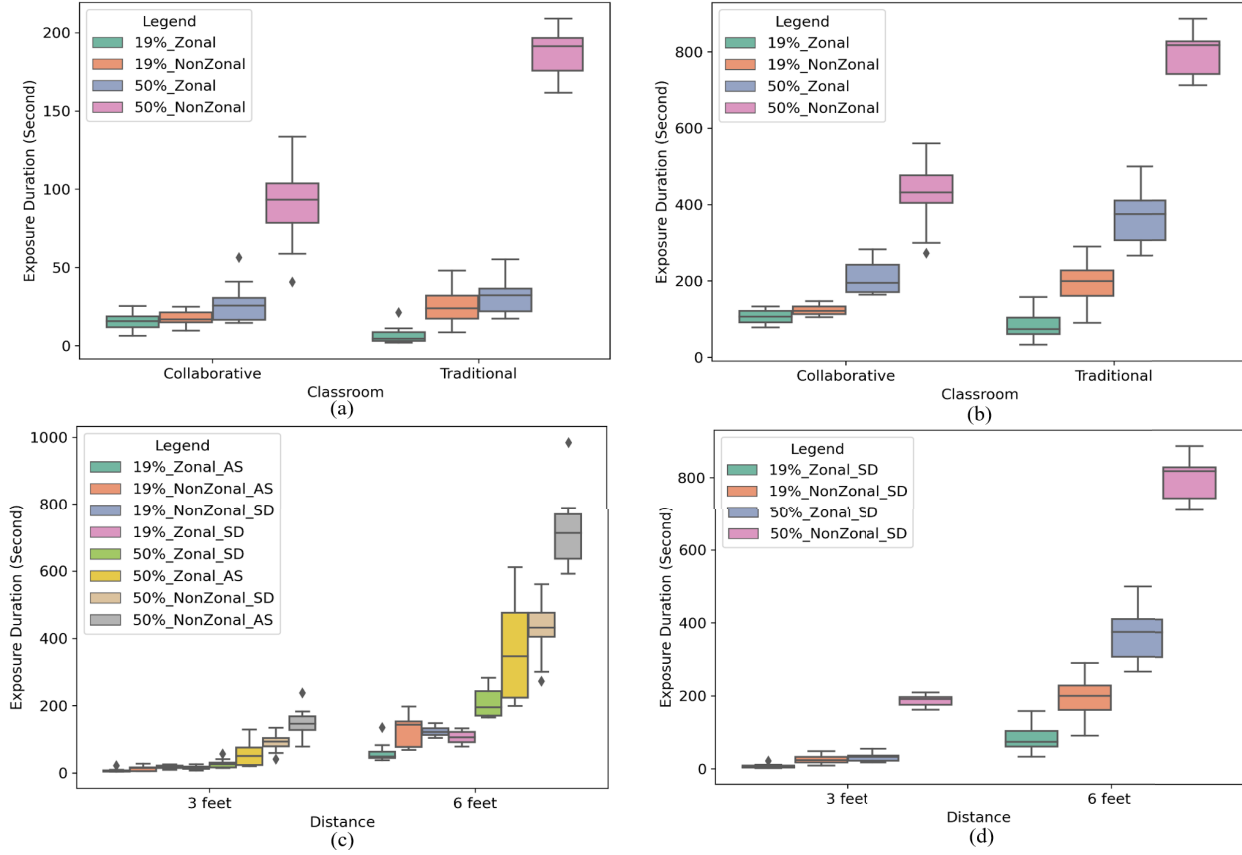


Fig. 10. Average exposure duration boxplot for (a) 0–3-ft distance, (b) 3–6-ft distance, (c) collaborative layout, and (d) traditional layout settings.

settings. This occurs due to the more streamlined movement of students in the traditional settings due to long desks, which ensures a natural queue during exit operation.

2) Average Exposure Duration: Safer operations of indoor activities cannot be achieved without considering the exposure-related metrics. Hence, this work utilizes and evaluates the average exposure duration of each student within two distance ranges: 0–3, and 3–6 ft. The exposure durations have been calculated for different classroom settings, exit policies, and seat selection policies. As shown in Fig. 10(a) exposure duration at 0–3 ft and (b) exposure duration at 3–6 ft, respectively, collaborative classrooms perform uniformly better than traditional settings at both distance ranges except for one combination (19% occupancy with zonal exit). Considering this combination, traditional classroom settings perform better due to the natural queue formed (guided by long desks) within the seating area. However, this benefit is less pronounced during higher occupancy (50%) and non-zonal exit policy due to more restricted pathways. With higher occupancy, wide and open pathways become more important to avoid congestion during non-zonal exit policy. In comparison to traditional settings during high congestion at the door/pathway areas, collaborative settings allow for more flexibility with more row opening toward the pathways, allowing the crowd to move more easily between the table gaps. This eventually helps in reducing the exposure time in collaborative settings during high occupancy.

Exposure duration at different distance buckets (0–3 and 3–6 ft) acknowledge higher risk associated with a non-zonal exit policy. From Fig. 10(c) collaborating settings and (d) traditional settings, clearly at a lower occupancy level (19%), exposure duration is not much affected by exit and seating policies in the 0–3-ft range. However, at the higher occupancy (50%) level, the zonal exit policy results in a considerably lower exposure duration compared to the non-zonal exit policy. This result validates pedestrian behavior where unregulated movement toward the exit door intuitively causes high exposure risk. Additionally, from Fig. 10(c), distinctively, our proposed SD seating policy causes a lower exposure duration at higher occupancy (50%) level. However, both SD and AS seating policies perform identically for lower occupancy (19%) level.

3) Average Number of Contact: In addition to the average exposure duration, the average contact number provides insights pertaining to the number of other students within the range. It is important to parallelly analyze the average contact number because the exposure duration for each student shows the cumulative exposure time. Hence average contact number provides the distribution of exposure time within the proximity of each agent. As shown in Fig. 11(a) collaborative settings and (b) traditional settings, the zonal policy facilitates the significant reduction of the average contact number. Intuitively, a non-zonal exit policy causes unregulated outward flow and thus leads to higher physical distancing violations, which in

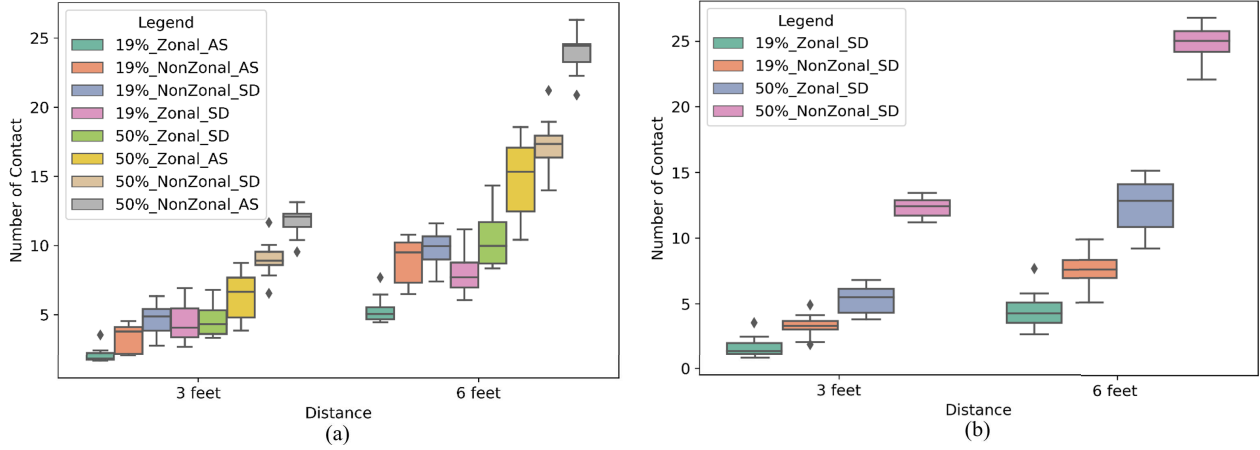


Fig. 11. Average contact number boxplot for (a) collaborative layout and (b) traditional layout settings.

turn would lead to a higher contact number. Hence, in order to ensure the safer operations of indoor activities, it is important to ensure the regulated flow of students using zonal exit policies. Furthermore, when the zonal exit policy is followed, the suggested SD seating policy ensures a smaller number of contacts at all distance ranges at 50% occupancy. This occurs due to higher penalties at the pathway and door side seats which ensures a minimum number of contacts between agents. The AS seating strategy, however, performs better with lower occupancy (19%). In contrast to SD seating, where students choose the seat furthest from the door, in AS policy students choose the seat closest to the door, resulting in shorter exposure duration and fewer contacts due to the faster exit operation.

Implementation of a zonal exit policy would lead to higher exit times as it increases the commute distance and time within the classroom. Hence, in terms of policymaking the appropriate tradeoff needs to be established between the safety and commutation to ensure optimal operations of the indoor spaces.

We tested our model by changing the percentage of people who follow the 6-ft physical distancing guideline to mimic the real-world scenario where some people may break the regulations because of ignorance or unwillingness. Users can set the percentage of agents who will follow the physical distancing rule from the simulation dashboard startup screen. For physical distancing follower percentage, we tested four different combinations (i.e., 100 percent, 80 percent, 60 percent, and 40 percent). The value 80 percent indicates that 80 percent of the classroom participants will adhere to the strict physical distancing requirement, while the remaining 20 percent are not restricted by the rule. We considered a higher occupancy level (50%), as well as a collaborative classroom layout as a fixed simulation setting.

As demonstrated in Fig. 12(a) number of contacts and (b) exposure duration boxplots, we were able to make some interesting observations by varying the physical distancing follower percentage. When 100% of the students obey the rule, the value for both the number of contacts and the exposure duration is fairly low. If we lower the proportion to 80%, both

the exposure duration and the number of contacts increased which is aligned with our intuition. However, if we decrease the percentage further (e.g., 60% and 40%), interestingly at 0–3-ft range number of contact and exposure duration does not change significantly. This behavior can be described from the point of view of a student's physical distancing circle who is supposed to be a rule follower. When everyone maintains the distance rule, no one, without exception, crosses the physical distancing circle (0–3 ft) of others (e.g., deadlock). However, if 20% of the students do not obey the rule, they may trespass into the distancing circle of another 20% of students (or more if the student interacts with multiple students at the very same time) who are willing to respect the rules. This may result in only 60% or less effective rule followers, despite the fact that the rule was modeled to be followed by 80% of the students. Similarly, if 60% of students are supposed to obey the rules, the number of effective rule followers will be less than planned. However, since 40% of students are not restricted by the rule, there will be a larger likelihood of contact amongst willing rule breakers. This could explain the possible equilibrium point in average contact number and contact time at the 60%, 40%, or lower rule follower levels.

In contrast, we have seen a declining trend in exposure duration at the 3–6-ft range as the rule breaker percentage rises. Some of the students who were previously at the 3–6-ft range will get closer to each other and will be within the 0–3-ft range as the percentage of rule followers decreases (e.g., from 100% to 80%). Because those contacts are now in the 0–3-ft time bucket, they will be removed from the 3–6-ft time bucket, and the exposure duration for that distance will be reduced. Exit time for the students can also be used to explain this behavior. When the number of students who follow the rules is reduced from 100% to 80%, 60%, and 40%, students leave the classroom faster, resulting in less time spent in exit operation. Because of the less exit time, eventually students spend less time within the 3–6-ft zone, and so exposure duration for that time bucket decreases.

4) Factor Effect Analysis: In this work, two independent variables namely, classroom occupancy and exit policy have been considered under four different scenarios to evaluate

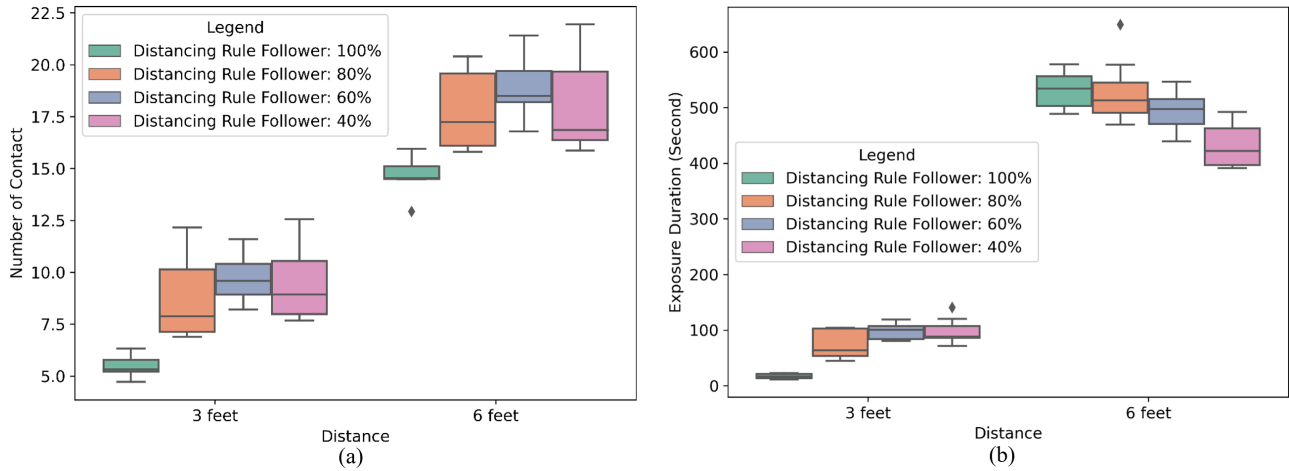


Fig. 12. Average (a) number of contacts and (b) exposure duration boxplots by varying physical distancing rule follower percentage.

the traditional layout of the classroom. A significant positive correlation was observed based on the correlation analysis between the exposure duration and the number of contacts ($r = 0.97, p < 0.01$). Furthermore, multivariate analysis of variance (MANOVA) was studied in order to test the main and interaction effects with the exposure duration and contact distance under the traditional classroom layout. We observed that, the classroom occupancy has a significant main effect [$F(1, 79) = 124.54, p < 0.01$]. Exit policies also demonstrated significant main effect [$F(1, 79) = 51.78, p < 0.01$]. It is also evident that there is a significant interaction effect between the allowable occupancy and exit policy [$F(1, 79) = 21.49, p < 0.01$], which indicates the importance of exit policies given a higher occupancy percentage of the classroom.

Fig. 13(a) shows the average exposure duration for traditional classroom layout within two distance ranges (0–3, and 3–6 ft) under different occupancy levels. Hence, it can be inferred that exit policies show significant differences when the maximum allowable occupancy of the classroom is higher.

For collaborative classrooms, we have conducted experiments to analyze the main effects and interaction effects using three different independent variables: classroom occupancy, exit policy, and seating policy. The response variable under consideration includes exposure duration, whereas contact distance was a covariate. Based on the correlation analysis, a significant positive correlation was observed between the number of contact and exposure duration ($r = 0.95, p < 0.01$). The multi-analysis of variance was conducted to test the main effects and interaction effects with the exposure duration. A significant main effect have been observed for classroom occupancy [$F(1, 159) = 138.20, p < 0.01$] and exit policy [$F(1, 159) = 40.17, p < 0.01$]. Similarly, significant interaction effect was observed between the classroom occupancy and exit policy [$F(1, 159) = 21.99, p < 0.01$]. Interestingly, a significant interaction effect between the occupancy and seat selection policy was also observed [$F(1, 159) = 19.54, p < 0.01$].

Based on the analysis for the collaborative classroom layout, it can be inferred that the exit policy and seat selection

policy play a crucial role in ensuring the safer operation of classroom activities. As shown in Fig. 13(b) and (c), significant reductions in the average exposure duration show that the zonal exit and the proposed SD seat selection policy makes a difference in the exposure, thus helpful in controlling the classroom infectious risk level under the collaborative classroom setting.

Another important aspect that needs to be investigated includes the type of classroom layout that a university should adopt given safety and logistics. Traditional and collaborative layouts, in combination with zonal exit, were found to help reduce exposure duration at 0–3 ft [see Fig. 13(d)]. At a distance of 3–6 ft, however, collaborative policy performs better as the occupancy levels increase [see Fig. 13(e)]. Here, the main effects and interaction effects for three factors namely, occupancy %, classroom type, and exit policy were tested to draw conclusions pertaining to the layout and policy requirements for the classroom operations. The three-way interaction effect was non-significant [$F(1, 159) = 2.49, p > 0.05$]. However, a significant interaction effect between classroom type and occupancy was observed [$F(1, 159) = 25.80, p < 0.01$].

C. Verification and Validation

The verification and validation is an iterative process that takes place throughout the development phase of any simulation study. Because the simulation models developed during this research work represent actual university facilities (e.g., classroom, meeting room, auditorium, office room, and dance class), significant time was spent visiting all of space, and documenting functional specifications (e.g., type of indoor space, number of doors, total capacity, room layout, class time, break time) and spatial information (e.g., facility size, number of desks and chairs, the gap between rows and columns, door position, teacher's corner position). Furthermore, the work in this article used the University of Arizona's "Interactive Floorplans" [48] platform to assess the spatial position of a facility, the number of connecting hallways and hallway

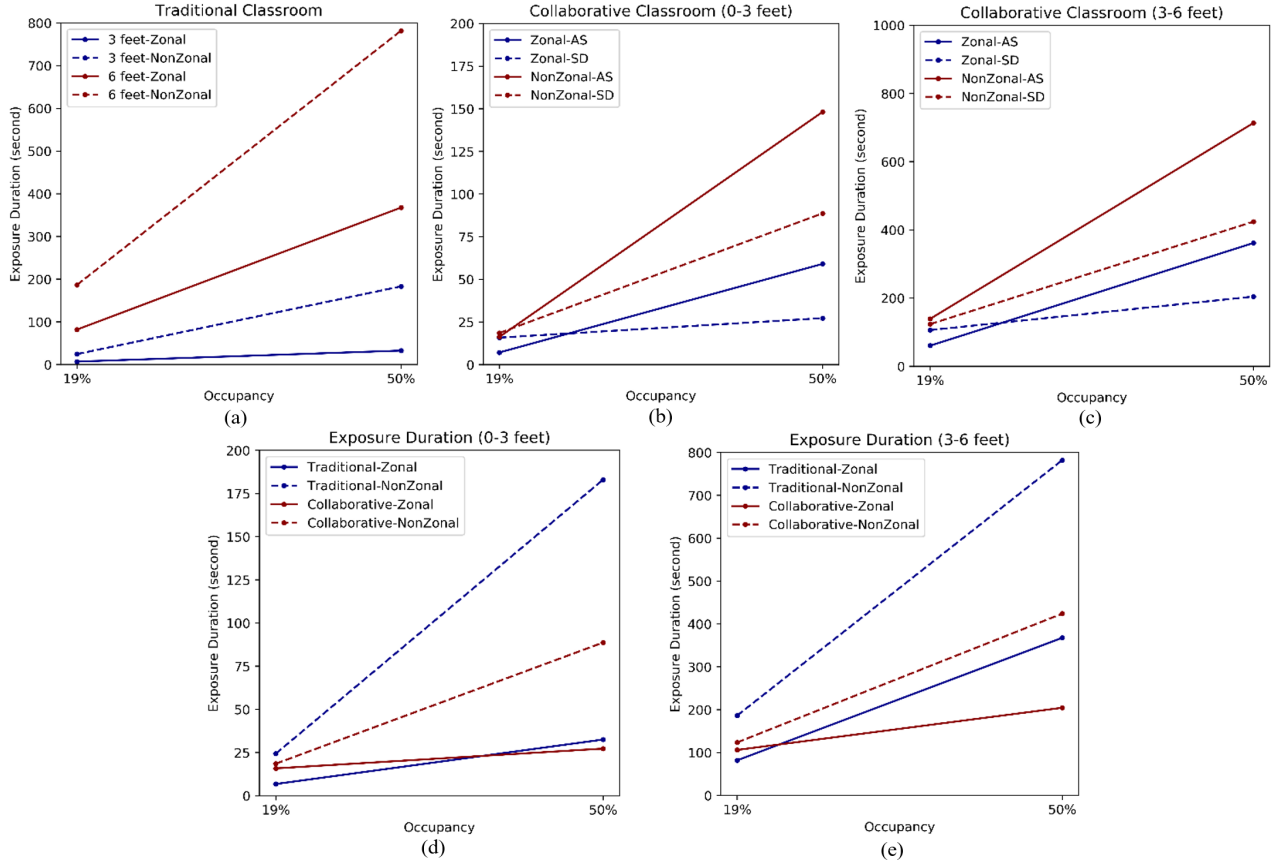


Fig. 13. Interaction effect in terms of exposure duration for (a) distance and exit policy with occupancy in traditional, seating and exit policy with occupancy at (b) 0–3 ft and (c) at 3–6 ft in collaborative, layout and exit policy with occupancy at (d) 0–3 ft and (e) at 3–6 ft distance.

dimensions, the number of floors, and the location of the staircase to accurately model incoming and outgoing pedestrians. Throughout the model development process, the models were constantly presented to the university facility management and the campus reopening authority to verify the collected data and solicit suggestions for model parameters and policy evaluation (e.g., entrance and exit policy, seating policy, and classroom occupancy policy).

As decision-makers and individuals intend to use the developed models to evaluate their decisions, they are highly concerned about the accuracy of the models. In this work, there were two types of results: a. mimicking real-world pedestrian dynamics and b. statistics (i.e., exit time, number of contacts, exposure duration). As previously stated, the developed models were constantly presented to the university facility management personnel, the campus reopening authority, a group of students, and research experts to verify and validate them and replicate realistic pedestrian movement within the indoor space. During the verification and validation process, valuable feedbacks were provided regarding certain irregular crowd motions, which we later identified as deadlock situations and resolved by implementing our deadlock detection and resolution algorithm (see Section III-F). After several iterations, the model development was completed, which was then used by stakeholders to evaluate different configurations of the indoor facility.

Due to university restrictions on in-person class attendance, testing the simulation statistics against any real data or recorded video during the COVID-19 pandemic was not possible. However, due to extensive verification and validation efforts with the campus experts as well as the availability of highly detailed data of the indoor facilities, the developed models are believed to be sufficiently valid and accurate to provide meaningful managerial insights in evaluating alternative policies and scenarios.

V. CONCLUSION AND FUTURE DIRECTIONS

In this work, we demonstrated a simulation for indoor facilities using a case study of a classroom environment. Thus, this work can serve as a foundation to incorporate disease propagation based on contact-caused risk within an indoor facility. This will facilitate in getting deeper insights on hotspots throughout the facility and identify the high-risk areas. The physical distancing and deadlock resolution mechanisms have been considered in this study to incorporate a high degree of realism in pedestrian behaviors. Furthermore, we have conducted model testing under the different entrance and exit policies, seating policies to reduce the contacts and exposure due to physical distancing violations. Different policies were assessed based on outputs depicting the logistics (e.g., exit time) and risk metrics (e.g., number of contact and

exposure duration). Based on the simulation results, it was suggested that utilizing a collaborative classroom with zonal exit policies leads to the significant reduction of exposure risk in a higher occupancy level. Moreover, implementing the proposed SD seat assignment approach played a crucial role in reducing the exposure duration. However, with a significantly lower occupancy level, the classroom layout did not play a significant role in reducing exposure risk levels.

This application can be used in K-12 schools across the country to ensure minimal student contact and a safer classroom environment. Furthermore, institutions (e.g., schools, colleges, universities, and offices), business owners (e.g., restaurants and groceries), and prayer hall authorities (e.g., mosque and church) can conduct different what-if analyses by rearranging the chairs, desks, and walkways to determine the best seating arrangement in terms of minimum contacts within the indoor space. Because of the high-fidelity simulation videos, this application may also be used to teach people how to properly enter, take a seat, and exit an indoor facility while adhering to policy (e.g., zonal versus non-zonal, physical distancing). This study can provide some basic takeaways for organizations that do not have the expertise to use this modeling technology. One is to implement SD seating policy, which can be readily accomplished by ensuring that the seats with the greatest distance from the doors are the first to be occupied, reducing recurrent contact between persons sitting near the doors. By designing zones in a large interior space, organizations may ensure a zonal exit strategy. Furthermore, everyone should conform to the physical distancing rules because if some students do not, they may come into contact with others who wish to follow the rules, lowering the effective rule follower percentage significantly.

This work can be extended in different dimensions. Detailed analysis of disease propagation within indoor spaces can be performed by incorporating the droplet and airborne transmission models. Key factors affecting droplet and airborne transmission, including breathing rate, agent's height and weight, classroom volume, class length, HVAC parameters, and mask-wearing percentages, would undoubtedly enhance the modeling and analysis capabilities within indoor spaces during a pandemic situation. Furthermore, while this work only considered a 3-ft physical distancing policy, this framework can be modified to incorporate different physical distancing recommendations based on the requirements. Although the policy choice depends on different factors, it is worth investigating to find the best combination of policies to make indoor safer in this pandemic situation. The outputs from the proposed work can be used to fit an appropriate meta-model, which can provide relevant input parameters for an organization-wide disease propagation model. Moreover, the proposed framework can be deployed to assess operations in other organizations such as manufacturing facilities, hospitals, and military bases. Additional features into the proposed system can be incorporated to provide an online decision support system for different stakeholders to provide a real-time assessment of the situation in particular indoor spaces.

REFERENCES

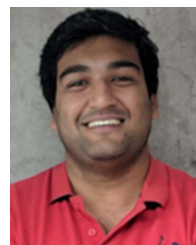
- [1] *COVID-19 Weekly Epidemiological Update*. Accessed: Jun. 07, 2021. [Online]. Available: <https://www.who.int/publications/m/item/weekly-epidemiological-update-on-covid-19—8-june-2021>
- [2] A. A. Volk, K. J. Brazil, P. Franklin-Luther, A. V. Dane, and T. Vaillancourt, "The influence of demographics and personality on COVID-19 coping in young adults," *Pers. Individual Differences*, vol. 168, Jan. 2021, Art. no. 110398, doi: [10.1016/j.paid.2020.110398](https://doi.org/10.1016/j.paid.2020.110398).
- [3] J. R. Goldstein and R. D. Lee, "Demographic perspectives on the mortality of COVID-19 and other epidemics," *Proc. Natl. Acad. Sci. USA*, vol. 117, no. 36, pp. 22035–22041, Sep. 2020, doi: [10.1073/pnas.2006392117](https://doi.org/10.1073/pnas.2006392117).
- [4] M. Monod *et al.*, "Age groups that sustain resurging COVID-19 epidemics in the United States," *Science*, vol. 371, no. 6536, Mar. 2021, doi: [10.1126/science.abe8372](https://doi.org/10.1126/science.abe8372).
- [5] S. Pokhrel and R. Chhetri, "A literature review on impact of COVID-19 pandemic on teaching and learning," *Higher Educ. Future*, vol. 8, no. 1, pp. 133–141, Jan. 2021, doi: [10.1177/2347631120983481](https://doi.org/10.1177/2347631120983481).
- [6] United Nations. (2020). *Policy Brief: Education During COVID-19 and Beyond*. Accessed: Jan. 18, 2021. [Online]. Available: https://www.un.org/development/desa/dspd/wp-content/uploads/sites/22/2020/08/sg_policy_brief_covid-19_and_education_august_2020.pdf
- [7] M. Kaffenberger, "Modelling the long-run learning impact of the COVID-19 learning shock: Actions to (more than) mitigate loss," *Int. J. Educ. Develop.*, vol. 81, Mar. 2021, Art. no. 102326, doi: [10.1016/j.ijedudev.2020.102326](https://doi.org/10.1016/j.ijedudev.2020.102326).
- [8] R. M. Viner *et al.*, "Reopening schools during the COVID-19 pandemic: Governments must balance the uncertainty and risks of reopening schools against the clear harms associated with prolonged closure," *Arch. Disease Childhood*, vol. 106, no. 2, pp. 111–113, Feb. 2021, doi: [10.1136/archdischild-2020-319963](https://doi.org/10.1136/archdischild-2020-319963).
- [9] N. N. C. House, S. Palissery, and H. Sebastian, "Corona viruses: A review on SARS, MERS and COVID-19," *Microbiol. Insights*, vol. 14, Jan. 2021, Art. no. 117863612110024, doi: [10.1177/11786361211002481](https://doi.org/10.1177/11786361211002481).
- [10] D. P. Oran and E. J. Topol, "Prevalence of asymptomatic SARS-CoV-2 infection," *Ann. Internal Med.*, vol. 173, no. 5, pp. 362–367, Sep. 2020, doi: [10.7326/M20-3012](https://doi.org/10.7326/M20-3012).
- [11] N. G. Davies *et al.*, "Age-dependent effects in the transmission and control of COVID-19 epidemics," *Nature Med.*, vol. 26, no. 8, pp. 1205–1211, Aug. 2020, doi: [10.1038/s41591-020-0962-9](https://doi.org/10.1038/s41591-020-0962-9).
- [12] D. K. Chu *et al.*, "Physical distancing, face masks, and eye protection to prevent person-to-person transmission of SARS-CoV-2 and COVID-19: A systematic review and meta-analysis," *Lancet*, vol. 395, Jun. 2020, Art. no. 10242, doi: [10.1016/S0140-6736\(20\)31142-9](https://doi.org/10.1016/S0140-6736(20)31142-9).
- [13] R. Dhand and J. Li, "Coughs and sneezes: Their role in transmission of respiratory viral infections, including SARS-CoV-2," *Amer. J. Respiratory Crit. Care Med.*, vol. 202, no. 5, pp. 651–659, Sep. 2020, doi: [10.1164/rccm.202004-1263PP](https://doi.org/10.1164/rccm.202004-1263PP).
- [14] N. H. L. Leung *et al.*, "Respiratory virus shedding in exhaled breath and efficacy of face masks," *Nature Med.*, vol. 26, no. 5, pp. 676–680, May 2020, doi: [10.1038/s41591-020-0843-2](https://doi.org/10.1038/s41591-020-0843-2).
- [15] World Health Organisation. (2020). *Coronavirus Disease (COVID-19) Advice for the Public: Mythbusters*. [Online]. Available: <https://www.who.int/emergencies/diseases/novel-coronavirus-2019/advice-for-public/myth-busters#5g%0Ahttps://www.who.int/>
- [16] U.S. Centers for Disease Control Prevention. (2020). *Social Distancing*. Accessed: Jan. 18, 2021. [Online]. Available: <https://www.cdc.gov/coronavirus/2019-ncov/prevent-getting-sick/social-distancing.html>
- [17] R. Koch Institute. *COVID-19 Situation Report 02.06.2020*. Accessed: Jan. 21, 2021. [Online]. Available: <https://corona.rki.de>
- [18] Scientific Advisory Group for Emergencies. *Update Paper Prepared by Environmental and Modelling Group (EMG) on Transmission of SARS-CoV-2 and Mitigating Measures*. Accessed: Jan. 11, 2021. [Online]. Available: <https://www.gov.uk/government/publications/transmission-of-sars-cov-2-and-mitigating-measures-update-4-june-2020>
- [19] N. R. Jones, Z. U. Qureshi, R. J. Temple, J. P. J. Larwood, T. Greenhalgh, and L. Bourouiba, "Two metres or one: What is the evidence for physical distancing in COVID-19?" *BMJ*, vol. 370, p. m3223, Aug. 2020, doi: [10.1136/bmj.m3223](https://doi.org/10.1136/bmj.m3223).

- [20] H.-Y. Cheng, S.-W. Jian, D.-P. Liu, T.-C. Ng, W.-T. Huang, and H.-H. Lin, "High transmissibility of COVID-19 near symptom onset," *medRxiv*, Jan. 2020, doi: [10.1101/2020.03.18.20034561](https://doi.org/10.1101/2020.03.18.20034561).
- [21] L. Zhong, "A dynamic pandemic model evaluating reopening strategies amid COVID-19," *PLoS ONE*, vol. 16, no. 3, Mar. 2021, Art. no. e0248302, doi: [10.1371/journal.pone.0248302](https://doi.org/10.1371/journal.pone.0248302).
- [22] W. J. Edmunds, "Finding a path to reopen schools during the COVID-19 pandemic," *Lancet Child Adolescent Health*, vol. 4, no. 11, pp. 796–797, Nov. 2020, doi: [10.1016/S2352-4642\(20\)30249-2](https://doi.org/10.1016/S2352-4642(20)30249-2).
- [23] L. Morawska *et al.*, "How can airborne transmission of COVID-19 indoors be minimised?" *Environ. Int.*, vol. 142, Sep. 2020, Art. no. 105832, doi: [10.1016/j.envint.2020.105832](https://doi.org/10.1016/j.envint.2020.105832).
- [24] D. Lewis, "Why indoor spaces are still prime COVID hotspots," *Nature*, vol. 592, no. 7852, Apr. 2021, pp. 22–25, doi: [10.1038/d41586-021-00810-9](https://doi.org/10.1038/d41586-021-00810-9).
- [25] S. W. X. Ong *et al.*, "Air, surface environmental, and personal protective equipment contamination by severe acute respiratory syndrome coronavirus 2 (SARS-CoV-2) from a symptomatic patient," *J. Amer. Med. Assoc.*, vol. 323, no. 16, pp. 1610–1612, Apr. 2020, doi: [10.1001/jama.2020.3227](https://doi.org/10.1001/jama.2020.3227).
- [26] A. T. Murray, "Planning for classroom physical distancing to minimize the threat of COVID-19 disease spread," *PLoS ONE*, vol. 15, no. 12, Dec. 2020, Art. no. e0243345, doi: [10.1371/journal.pone.0243345](https://doi.org/10.1371/journal.pone.0243345).
- [27] M. Salari, R. J. Milne, C. Delcea, L. Kattan, and L.-A. Cotfas, "Social distancing in airplane seat assignments," *J. Air Transp. Manage.*, vol. 89, Oct. 2020, Art. no. 101915, doi: [10.1016/j.jairtraman.2020.101915](https://doi.org/10.1016/j.jairtraman.2020.101915).
- [28] C. Delcea, R. J. Milne, and L.-A. Cotfas, "Determining the number of passengers for each of three reverse pyramid boarding groups with COVID-19 flying restrictions," *Symmetry*, vol. 12, no. 12, p. 2038, Dec. 2020, doi: [10.3390/sym12122038](https://doi.org/10.3390/sym12122038).
- [29] T. Harweg, D. Bachmann, and F. Weichert, "Agent-based simulation of pedestrian dynamics for exposure time estimation in epidemic risk assessment," 2020, *arXiv:2007.04138*. [Online]. Available: <http://arxiv.org/abs/2007.04138>
- [30] A. Mohammadi, M. T. U. Chowdhury, S. Yang, and P. Y. Park, "Developing levels of pedestrian physical distancing during a pandemic," *Saf. Sci.*, vol. 134, Feb. 2021, Art. no. 105066, doi: [10.1016/j.ssci.2020.105066](https://doi.org/10.1016/j.ssci.2020.105066).
- [31] T.-C. Row and Y.-L. Pan, "Maximally permissive deadlock prevention policies for flexible manufacturing systems using control transition," *Adv. Mech. Eng.*, vol. 10, no. 7, Jul. 2018, Art. no. 1687814018787406, doi: [10.1177/1687814018787406](https://doi.org/10.1177/1687814018787406).
- [32] E. A. Nasr, A. M. El-Tamimi, A. Al-Ahmari, and H. Kaid, "Comparison and evaluation of deadlock prevention methods for different size automated manufacturing systems," *Math. Problems Eng.*, vol. 2015, Sep. 2015, Art. no. 537893, doi: [10.1155/2015/537893](https://doi.org/10.1155/2015/537893).
- [33] M.-L. Xiao, Y. Chen, M.-J. Yan, L.-Y. Ye, and B.-Y. Liu, "Simulation of household evacuation in the 2014 Ludian earthquake," *Bull. Earthq. Eng.*, vol. 14, no. 6, pp. 1757–1769, Jun. 2016, doi: [10.1007/s10518-016-9887-6](https://doi.org/10.1007/s10518-016-9887-6).
- [34] H. Xi, Y.-J. Son, and S. Lee, "An integrated pedestrian behavior model based on extended decision field theory and social force model," in *Proc. Winter Simulation Conf.* IEEE, Dec. 2010, doi: [10.1109/WSC.2010.5679108](https://doi.org/10.1109/WSC.2010.5679108).
- [35] J. Yuyang and M. Hongyan, "Study on evacuation simulation of medical pension building based on anylogic," in *Proc. Chin. Control Decis. Conf.*, 2018, pp. 2307–2312, doi: [10.1109/CCDC.2018.8407511](https://doi.org/10.1109/CCDC.2018.8407511).
- [36] J. Zhou, Y. Guo, S. Dong, M. Zhang, and T. Mao, "Simulation of pedestrian evacuation route choice using social force model in large-scale public space: Comparison of five evacuation strategies," *PLoS ONE*, vol. 14, no. 9, Sep. 2019, Art. no. e0221872, doi: [10.1371/journal.pone.0221872](https://doi.org/10.1371/journal.pone.0221872).
- [37] D. Helbing, I. Farkas, and T. Vicsek, "Simulating dynamical features of escape panic," *Nature*, vol. 407, no. 6803, pp. 487–490, Sep. 2000, doi: [10.1038/35035023](https://doi.org/10.1038/35035023).
- [38] S. C. Newbold, D. Finnoff, L. Thunström, M. Ashworth, and J. F. Shogren, "Effects of physical distancing to control COVID-19 on public health, the economy, and the environment," *Environ. Resour. Econ.*, vol. 76, no. 4, pp. 705–729, Aug. 2020, doi: [10.1007/s10640-020-00440-1](https://doi.org/10.1007/s10640-020-00440-1).
- [39] *6 Feet of Social Distancing Best, But Even 3 Feet Should Help: Study* USNEWS, Washington, DC, USA, 2020.
- [40] M. P. van den Berg *et al.*, "Effectiveness of 3 versus 6 ft of physical distancing for controlling spread of coronavirus disease 2019 among primary and secondary students and staff: A retrospective, statewide cohort study," *Clin. Infectious Diseases*, 2021, doi: [10.1093/cid/ciab230](https://doi.org/10.1093/cid/ciab230).
- [41] Jonathan Ponciano. (Mar. 2021). *Fauci Says Three-Feet Social Distancing May Suffice To Reopen Schools*. Accessed: Mar. 13, 2021. [Online]. Available: <https://www.forbes.com/sites/jonathanponciano/2021/03/14/fauci-says-three-feet-social-distancing-may-suffice-to-reopen-schools/?sh=56d0f8312cf3>
- [42] C. D. Fryar, Q. Gu, C. L. Ogden, and K. M. Flegal, "Anthropometric reference data for children and adults: United States, 2011–2014," in *Vital and Health Statistics. Series 3, Analytical Studies*, no. 39. 2016.
- [43] F. Blume, R. Göllner, K. Moeller, T. Dresler, A.-C. Ehlis, and C. Gawrilow, "Do students learn better when seated close to the teacher? A virtual classroom study considering individual levels of inattention and hyperactivity-impulsivity," *Learn. Instruct.*, vol. 61, pp. 138–147, Jun. 2019, doi: [10.1016/j.learninstruc.2018.10.004](https://doi.org/10.1016/j.learninstruc.2018.10.004).
- [44] *Pedestrian Library*. Accessed: Jul. 17, 2021. [Online]. Available: <https://www.anylogic.com/features/libraries/pedestrian-library/>
- [45] K. Magzhan and H. Jani, "A review and evaluations of shortest path algorithms," *Int. J. Sci. Technol. Res.*, vol. 2, no. 6, pp. 99–104, 2013.
- [46] Office of Governor Doug Ducey. (2020). *Further Action to Reverse COVID-19 Spread in Arizona*. Accessed: Jan. 18, 2021. [Online]. Available: <https://azgovernor.gov/governor/news/2020/06/further-action-reverse-covid-19-spread-arizona#:~:text=Prohibiting%20mass%20gatherings%20statewide,than%2050%20people%20are%20prohibited>
- [47] T. K. Hui. (Mar. 2021). *NC Lawmakers Vote for More Spectators at High School and College Games, Graduations*. Accessed: Mar. 13, 2021. [Online]. Available: <https://www.newsobserver.com/news/politics-government/article249669078.html>
- [48] *Interactive Floorplan*. Accessed: Jul. 18, 2021. [Online]. Available: <https://interactivefloorplans.arizona.edu>



Md Tariqul Islam received the B.Sc. degree in industrial and production engineering from Bangladesh University of Engineering and Technology, Dhaka, Bangladesh, in 2016. He is currently pursuing the Ph.D. degree with the Department of Systems Industrial and Engineering, The University of Arizona, Tucson, AZ, USA.

Before starting his Ph.D. degree, he worked as a Planning Zone Planner and a Supply Production Planner with Decathlon France. His research interest includes data driven simulation-based decision support systems.



Saurabh Jain received the B.Tech. degree in mechanical engineering from India, in 2015, and the M.S. degree in industrial engineering from The University of Arizona, Tucson, AZ, USA, in 2017, where he is currently pursuing the Ph.D. degree with the Department of Systems Industrial and Engineering.

He has authored and coauthored published papers in different application domains at journals and conferences of national and international repute. His research interests include applied simulation modeling and analysis for large-scale systems.

Mr. Jain is also a member of the Institute of Operation Research and Management Sciences (INFORMS), the Institute of Industrial and Systems Engineers (IIE), the Society for Modeling Simulation International, and the Society for Simulation in Healthcare.



Yijie Chen received the B.S. degree in psychology from Zhejiang University, Hangzhou, China, in 2017. She is currently pursuing the Ph.D. degree with the Department of Systems Industrial and Engineering, The University of Arizona, Tucson, AZ, USA.

Her research interests include computational modeling and simulation of human cognitive behaviors and the optimization of systems to improve efficiency and reduce the risk of human users.



Bijoy Dripta Barua Chowdhury is currently pursuing the Ph.D. degree with the Department of Systems Industrial and Engineering, The University of Arizona, Tucson, AZ, USA.

Before starting his Ph.D. degree, he has served as a Lecturer for the Department of Industrial and Production Engineering, Bangladesh University of Engineering and Technology, Dhaka, Bangladesh. He has coauthored several manuscripts in journals and conference proceedings. His research interests include designing and developing the dynamic data-driven indoor localization systems for workflow and layout optimization.

Mr. Chowdhury is also a member of the Institute of Operation Research and Management Sciences and the Institute of Industrial and Systems Engineers. He received the IISE Annual Meeting Best Track Paper Award.



Young-Jun Son (Member, IEEE) is currently a Professor and the Department Head of Systems and Industrial Engineering with The University of Arizona, Tucson, AZ, USA.

He has authored/coauthored over 100 journal articles and 100 conference papers. His research interests include modeling and control of complex manufacturing and service enterprises, and distributed federation of multi-paradigm simulations. His research activities have been funded by National Science Foundation (NSF), Air Force Office of Scientific Research (AFOSR), Department of Transportation (DOT), DOE/AZ Commerce Authority, United States Department of Agriculture (USDA), National Institute of Standards and Technology (NIST), Sandia National Laboratories, the Science Foundation Arizona, Boeing, Samsung, Motorola, Raytheon, Tucson Electric Power, and Microsoft.

Prof. Son is also a fellow of the Institute of Industrial and Systems Engineers (IISE). He received the Society of Manufacturing Engineers (SME) 2004 Outstanding Young Manufacturing Engineer (ME) Award, the IIE 2005 Outstanding Young Industrial Engineer (IE) Award, the IISE Annual Meeting Best Paper Award in 2005, 2008, 2009, 2016, 2018, and 2019, and Best Paper of the Year Award in 2007 from *International Journal of Industrial Engineering: Theory, Applications, and Practice*. He has served as the Co-Program Chair for Industrial and Systems Engineering Research Conference (ISERC), 2007 and the General Chair for Institute for Operations Research and the Management Sciences (INFORMS) Annual Meeting 2018 and the Winter Simulation Conference 2019. He is also a Department Editor of *IISE Transactions*, on the editorial board for seven additional journals.